

## Low-temperature sintering of (U,Pu)O<sub>2</sub> MOX in mild oxidative conditions

Boshoven, Jacobus; Vigier, Jean François; Pöml, Philipp; Ndiaye, Abibatou; Morel, Bertrand; Konings, Rudy J.M.; Popa, Karin; Cologna, Marco

**DOI**

[10.1016/j.jnucmat.2025.155800](https://doi.org/10.1016/j.jnucmat.2025.155800)

**Publication date**

2025

**Document Version**

Final published version

**Published in**

Journal of Nuclear Materials

**Citation (APA)**

Boshoven, J., Vigier, J. F., Pöml, P., Ndiaye, A., Morel, B., Konings, R. J. M., Popa, K., & Cologna, M. (2025). Low-temperature sintering of (U,Pu)O<sub>2</sub> MOX in mild oxidative conditions. *Journal of Nuclear Materials*, 610, Article 155800. <https://doi.org/10.1016/j.jnucmat.2025.155800>

**Important note**

To cite this publication, please use the final published version (if applicable). Please check the document version above.

**Copyright**

Other than for strictly personal use, it is not permitted to download, forward or distribute the text or part of it, without the consent of the author(s) and/or copyright holder(s), unless the work is under an open content license such as Creative Commons.

**Takedown policy**

Please contact us and provide details if you believe this document breaches copyrights. We will remove access to the work immediately and investigate your claim.



# Low-temperature sintering of (U,Pu)O<sub>2</sub> MOX in mild oxidative conditions

Jacobus Boshoven<sup>a</sup>, Jean-François Vigier<sup>a, \*id</sup>, Philipp Pöml<sup>a</sup>, Abibatou Ndiaye<sup>b</sup>,  
Bertrand Morel<sup>c</sup>, Rudy J.M. Konings<sup>a, d</sup>, Karin Popa<sup>a, \*id</sup>, Marco Cologna<sup>a, \*id</sup>

<sup>a</sup> European Commission, Joint Research Centre (JRC), Karlsruhe, Germany

<sup>b</sup> ORANO Projects, MELOX, Les Tourettes, D138A, 30200, Chusclan, France

<sup>c</sup> ORANO Support, 92320 Chatillon, France

<sup>d</sup> Faculty of Applied Sciences, Radiation Science & Technology Department, Delft University of Technology, Mekelweg 15, Delft 2629JB, the Netherlands

## ARTICLE INFO

### Keywords:

MOX  
Sintering  
Nuclear fuel  
Diffusion

## ABSTRACT

We compare typical reductive sintering conditions for U, Pu mixed oxides (4 h at 1700 °C in Ar/6 % H<sub>2</sub> + 1200 ppm H<sub>2</sub>O) with lower temperature and mildly oxidative conditions (2 h at 1200 °C in CO/CO<sub>2</sub> = 1/9) and report on the resulting microstructures and homogeneity. We show that lower temperature and mildly oxidative conditions, without cover gas change, can give close-to stoichiometric, crack-free MOX pellets with a relative density of ~ 95 %, and we propose ways to improve the homogenisations of PuO<sub>2</sub> and UO<sub>2</sub> and increase the grain size.

## 1. Introduction

Uranium-plutonium mixed oxide (MOX) pellets are currently used as fuel in several nuclear reactors, as a way to reutilise plutonium produced during commercial operation [1,2]. They are also the reference fuel for most European fast neutron reactor demonstrators and prototypes [3]. Like UO<sub>2</sub>, MOX fuel is manufactured by ceramic powder technologies, involving three steps, (i) powder production, (ii) forming of green pellets and (iii) sintering. This last step is particularly energivorous, as it requires reaching temperatures in the order of 1700 °C over several hours. Hydrogen and optionally traces of water are used in the cover gas to avoid phase transformations and to set the final oxygen to metal ratio to the desired values, typically between 1.97 and 2.00. A reduction of the sintering temperature could increase the production sustainability, not only by decreasing the energy consumption, as well as reducing the cost and increasing the durability of the furnaces. This may be achieved by tackling the main variables affecting the sintering rate (Fig. 1): (i) reducing the powder particle size and distribution [4] (ii) applying external driving forces, as done in pressure assisted sintering techniques [5], or (iii) increasing the diffusion coefficient of the slowest (rate-limiting) species (in fluorite-type oxides, the diffusivity of the cation in the face-centred cubic sublattice is much lower than that of oxygen in the simple cubic sublattice [6]).

This last approach is particularly appealing for UO<sub>2</sub> and MOX, as the metal self-diffusion coefficient (D) increases by orders of magnitude

when increasing the oxygen stoichiometry above 2 - a relationship of  $D_U \propto X^2$  was suggested for UO<sub>2+x</sub> [7]. The extent of hyper-stoichiometry can be conveniently set by fixing the oxygen partial pressure of the processing gas during sintering, for example using appropriate mixtures of CO, CO<sub>2</sub>, H<sub>2</sub> or H<sub>2</sub>O [8].

This approach has been shown to decrease the sintering temperature from ~1700 °C to ~1100 °C and reduce significantly the production time. It is known as *low temperature sintering* (LTS), [9–11], *oxidative sintering* [12], or *NUKUSI* process (from the German Niedrigtemperatur-Kurzzeit-Sintern, translatable as “low-temperature, short-time sintering”), and used by Kraftwerk Union AG to produce 50 tons of UO<sub>2</sub> pellets for irradiation [12–14].

One of the drawbacks of the oxidative sintering is the need to change the atmosphere during processing, to reduce hyperstoichiometric UO<sub>2+x</sub> to UO<sub>2.00</sub> [15]. Another peculiarity is the need to control the solarisation phenomenon - a form of growth of grains and closed pores and concomitant de-sintering, or de-densification [16], which can be either seen as a drawback, or conveniently used to tailor the density, closed porosity, and grain size distribution [12,17].

The low-temperature hyperstoichiometric sintering of MOX is less reported in the open literature than UO<sub>2</sub>. Kutty et al. performed sintering studies by dilatometry of UO<sub>2</sub>, UO<sub>2</sub>–20 % PuO<sub>2</sub>, UO<sub>2</sub>–50 % PuO<sub>2</sub>, UO<sub>2</sub>–76 % PuO<sub>2</sub> and PuO<sub>2</sub>, showing that an oxidising atmosphere lowers the onset temperature for densification for MOX [18,19], while pure PuO<sub>2</sub> sinters better in Ar–8 % H<sub>2</sub> compared to CO<sub>2</sub> [20]. Recently, Miranda

\* Corresponding authors.

E-mail address: [marco.cologna@ec.europa.eu](mailto:marco.cologna@ec.europa.eu) (M. Cologna).

<https://doi.org/10.1016/j.jnucmat.2025.155800>

Received 21 February 2025; Received in revised form 27 March 2025; Accepted 31 March 2025

Available online 1 April 2025

0022-3115/© 2025 The Authors. Published by Elsevier B.V. This is an open access article under the CC BY license (<http://creativecommons.org/licenses/by/4.0/>).

et al. [21], performed a dilatometry study of  $U_{0.89}Pu_{0.11}O_{2+x}$  MOX fuel in a well-defined oxygen partial pressure (Ar + 4 vpm  $O_2$ ), and observed significant swelling above 1200 °C, with development of the typical solarised microstructures. The pressure of the gas trapped in the closed porosity is responsible for swelling, which counteracts the intrinsic sintering pressure. Miranda et al. convincingly identified this gas as the oxygen released during reduction of U and Pu oxides at higher temperatures, and not CO or  $CO_2$  as previously believed [21]. Barzati et al. [22], studied the solid solution formation in the  $U_{0.7}Pu_{0.3}O_{2+x}$  system at 1400 °C, found no reaction in He + 5 %  $H_2$ , and complete interdiffusion by increasing the oxygen partial pressure with water vapour. Using an excessively high oxygen partial pressure, gave low-quality pellets, because of solarisation and fracturing induced by phase changes.

Here we compare conventional sintering conditions for MOX (1700 °C in Ar/ $H_2$ / $H_2O$ ) with low-temperature (1200 °C), mildly oxidative conditions, and we report on the resulting microstructures and homogeneity. We show that lower temperature and mildly oxidative conditions, in  $CO/CO_2 = 1/9$  without gas change, can give close-to stoichiometric, crack-free MOX pellets with high density, and we propose ways to improve the homogenisations of  $PuO_2$  and  $UO_2$  and increase the grain size.

## 2. Experimental

### 2.1. Sample preparation

The starting uranium oxide powder was a commercial powder (Cogema TU2) with an average stoichiometry of  $UO_{2.12}$ , granules in the order of 10  $\mu m$  and primary particles in the order of 0.2–0.3  $\mu m$ . The plutonium oxide powder was  $PuO_{2.00}$  produced from oxalate precipitation, thus presenting the typical platelet morphology of several  $\mu m$  length. A more detailed characterisation is given elsewhere [4].

The feed powder mixture with a target composition of 0.11 Pu/(Pu + U) was prepared by dry vibratory milling (Retsch MM301) by adding the powders (2.438 g  $PuO_2$  and 19.692 g  $UO_2$ ) and three 12 mm diameter zirconia balls to a 25 ml zirconia jar. The mixture was milled for 2.5 h at a frequency of 15  $s^{-1}$  and 5 h at 20  $s^{-1}$  with 4 cooling breaks in total.

The density of the powders was measured by pouring the powder in a 10 ml glass cylinder and measuring the weight and the volume of the “as poured” powder (bulk density) and after gently shaking and tapping the cylinder until the powder volume showed no further decrease (tap density).

The milled powder without any additives was pressed at 405 MPa in a bi-directional press (Lauffer VIUG16), in 7.2 mm diameter dies lubricated on the surface with zinc stearate, into several green pellets (h ~ 5.8 mm) and disks (h ~ 1.4 mm) with a relative density of 69.7 % (the theoretical density (TD) of the solid mixture was estimated at 11.01  $g \cdot cm^{-3}$ ).

The green bodies were sintered either in “reductive” or “oxidising atmosphere”. The reductive sintering took place in a metallic furnace (Degussa VSL10/18) on a molybdenum tray, in flowing Ar + 6 %  $H_2$

moisturized with 1200 ppm of water vapour. The moisturized gas was used only from 600 °C, to prevent possible oxidation of the molybdenum at high oxygen potential at lower temperatures. Heating and cooling rates were 200 °C/h. The sintering schedule was as follows: heating to 600 °C in Ar/ $H_2$ , addition of 1200 ppm  $H_2O$  and dwell for 2 h, heating to 1700 °C and dwell for 4 h, cooling to 600 °C, switching-off of moisture and 1 h dwell in dry Ar/ $H_2$ , cooling to room temperature.

Oxidative sintering was performed in an alumina tubular furnace (AET) on an alumina tray at 1200 °C for 2 h. Heating and cooling rates were 200 °C/min. The furnace was flushed with a 10/90 mixture of carbon monoxide and carbon dioxide (BASI) with following specifications: 9.934 vol % CO (99.9 % purity) and rest  $CO_2$  (99.995 purity). After the oxidative sintering, some samples were re-annealed in the same gas as the reductive sintering (Ar + 6 %  $H_2$  + 1200 ppm  $H_2O$ ) at 600 °C for 2 h.

Green and sintered densities were measured geometrically, by measuring the weights on a balance (KERN PCB350) and the diameter and the height with a micrometer (Mitutoyo QuickMike), and with the Archimedes method for the sintered samples only, using a Sartorius BP211D balance equipped with a hydrostatic density kit.

### 2.2. Characterization techniques

The samples were analysed with a Bruker D8 X-ray diffractometer in a Bragg–Brentano configuration with a curved Ge monochromator (1,1,1), a copper tube (40 kV, 40 mA), equipped with a LinxEye position sensitive detector. Fragments of sintered pellets were pulverised in a mortar and deposited on a silicon wafer with a few drops of isopropanol. Profile refinement and structural analyses were performed with the JANA 2006 software suite.

The O/M ratio was measured by thermogravimetric analysis (TGA) with an oxidation/reduction procedure, adapted from ASTM C1817–16 to heating in a thermobalance. A fragment from the sintered pellets weighting > 100 mg was placed in a pre-treated  $Al_2O_3$  crucible and inserted in a TGA (Netzsch 449C) and subjected to the following schedule, with a gas flow of 60 ml/min: (i) heating in Ar at 10 °C/min to 900 °C, and 10 min isotherm, (ii) switching gas to air for one minute, (iii) switching again to argon for 10 min, (iv) switching to Ar/ $H_2$  and keeping the temperature at 900 °C for 160 min, and finally cooling.

The Pu/(U+Pu) ratio of the sintered pellets was measured by IDMS (Isotopic Dilution Thermal Ionisation Mass Spectrometry) using a Triton from Thermo Fisher Scientific GmbH.

Scanning Electron Microscopy (SEM) images were obtained with a Philips/FEI™ XL40 SEM placed inside a glovebox. The grain size was measured on the “as sintered” surface with the line intercept method without correction factor, using 4 SEM images and a minimum of 8 lines.

Electron micro probe analyzer (EPMA) measurements were carried out using a shielded Cameca SX100R equipped with four WDS spectrometers. The device was operated at an acceleration potential of 25 kV and a beam current of 100 nA. The 512×512  $\mu m$  maps are stage scan maps with a pixel dwelling time of 100 ms and 256×256 pixels. The

$$\dot{\rho} = \frac{f(\rho, geom)}{T} \cdot \frac{1}{d^m} \cdot D_0 e^{-\frac{Q_a}{RT}} \cdot \left( g \frac{\gamma_{SV}}{\lambda} + P_E \right)$$

**Fig. 1.** The variables affecting the sintering rate, where  $f$  is a function of the density ( $\rho$ ) and of the geometry, and includes mechanism-dependent constant terms,  $d$  is the particle size,  $m$  is a mechanism-dependent exponent ( $m = 2$  for volume diffusion-controlled sintering, and  $m = 3$  for grain boundary diffusion-controlled sintering),  $D_0$  is the pre-exponential factor of the diffusion coefficient of the slowest species along the fastest path, with activation energy  $Q_a$ . The last term represents the driving force, which is given by the sum of the effective external pressure,  $P_E$  (which is 0 for free sintering) and the intrinsic sintering pressure ( $g \gamma_{SV}/\lambda$ ), where  $g$  is a geometric term,  $\lambda$  a geometric scale of the microstructure, typically  $d$  or the pore radius.



**Table 2**

Cell parameter  $a_0$  from XRD analysis and calculated phase amounts and compositions using the Vegard's law between  $\text{UO}_{2.00}$  and  $\text{PuO}_{2.00}$ .

Sintering conditions	Phase	Amount	$a_0$ (Å)	Composition
1700 °C in Ar/H <sub>2</sub> + H <sub>2</sub> O	1	58.2 %	5.4670 (2)	(U <sub>0.94</sub> Pu <sub>0.06</sub> ) O <sub>2</sub>
	2	41.8 %	5.4594 (2)	(U <sub>0.84</sub> Pu <sub>0.16</sub> ) O <sub>2</sub>
	weighted av.		5.4638	(U <sub>0.90</sub> Pu <sub>0.10</sub> ) O <sub>2</sub>
1200 °C in CO/CO <sub>2</sub>	1	96.3 %	5.4668 (2)	(U <sub>0.94</sub> Pu <sub>0.06</sub> ) O <sub>2</sub>
	2	3.7 %	5.3989 (6)	(U <sub>0.03</sub> Pu <sub>0.97</sub> ) O <sub>2</sub>
	weighted av.		5.4644	(U <sub>0.90</sub> Pu <sub>0.10</sub> ) O <sub>2</sub>
1200 °C in CO/CO <sub>2</sub> and 600 °C in Ar/H <sub>2</sub> + H <sub>2</sub> O	1	96.7 %	5.4664 (2)	(U <sub>0.93</sub> Pu <sub>0.07</sub> ) O <sub>2</sub>
	2	3.3 %	5.3986 (6)	(U <sub>0.02</sub> Pu <sub>0.98</sub> ) O <sub>2</sub>
	weighted av.		5.4641	(U <sub>0.90</sub> Pu <sub>0.10</sub> ) O <sub>2</sub>

additional reduction step of the oxidative sintered pellets did not change the oxygen content, as can be concluded also from the unchanged lattice parameter.

Microstructures of the pellets are given in Fig. 4 ("as sintered" free surface) and Fig. 5 (fracture surface). Since the low-temperature annealing at 600 °C did not change the microstructure, only one sample is reported for the oxidative sintering. The mean grain size evaluated on the surface is  $2.3 \pm 0.5 \mu\text{m}$  and  $1.3 \pm 0.2 \mu\text{m}$ , for the reductive and oxidative sintered samples, respectively. The pellets sintered in reducing gas atmosphere show less porosity (Fig. 5, left), but the pore size is larger than the pellets sintered in oxidizing gas atmosphere (Fig. 5, right).

The U and Pu distribution as measured by EMPA is shown in Fig. 6. Both samples show spots with higher concentration of Pu. Such spots, with sizes below  $10 \mu\text{m}$ , are homogeneously distributed within the microstructure. Clearly, the inter-diffusion for the sample sintered at 1200 °C in oxidative conditions has been less effective, and more spots rich in Pu are visible.

#### 4.4. Discussion

When sintering is conducted in a buffer gas, such as a CO and CO<sub>2</sub> mixture at high temperature, the following equilibrium is rapidly reached, e.g. [23]:



The oxygen partial pressure in the gas, for a fixed CO to CO<sub>2</sub> ratio in

the inlet gas, can be determined from the equilibrium constant,  $K_C$ :

$$K_C = \frac{P_{\text{CO}_2}}{P_{\text{CO}}(p_{\text{O}_2})^{1/2}} \quad (2)$$

and

$$K_C = e^{-\left(\frac{\Delta G_c^0}{RT}\right)} \quad (3)$$

Where  $\Delta G_c^0$  is the standard-state Gibbs-energy change of the reaction in Eq. (1), and thus:

$$\Delta G_c^0 = \Delta H_c^0 - T\Delta S_c^0 \quad (4)$$

Where T is the temperature,  $\Delta H_c^0$  the standard enthalpy change ( $-282.4 \text{ kJ/mol}$ ) and  $\Delta S_c^0$  the standard entropy change ( $-86.8 \text{ J/(mol}\cdot\text{K)}$ ) [23]. The oxygen potential of the gas mixture can be calculated from the oxygen partial pressure as:

$$\Delta G_{\text{O}_2} = RT \ln p_{\text{O}_2} \quad (5)$$

In a similar way, the oxygen partial pressure set by the water/hydrogen buffer gas, was calculated for the reaction



with  $\Delta H_c^0 = -246.44 \text{ kJ/mol}$  and  $\Delta S_c^0 = -54.81 \text{ J/(mol}\cdot\text{K)}$  [24].

The oxygen partial pressure and potential of the selected buffer gases are given in Fig. 7. The used atmosphere of Ar/H<sub>2</sub>/H<sub>2</sub>O sets the oxygen potential at 1700 °C to  $-405 \text{ kJ/mol}$ , and at 600 °C to  $-454 \text{ kJ/mol}$ , while CO/CO<sub>2</sub> sets the oxygen potential at 1200 °C to  $-255 \text{ kJ/mol}$  and at 600 °C to  $-381 \text{ kJ/mol}$ .

The oxidative conditions chosen here are milder compared to other results reported in the literature. Miranda [21], sintered 11 % Pu-MOX in Ar + 4 vpm O<sub>2</sub> up to 1540 °C, which corresponds to an oxygen potential of  $-187 \text{ kJ/mol}$  at 1540 °C and  $-90 \text{ kJ/mol}$  at 600 °C. In such conditions, the experimentally measured O/M ratio achieved a maximum of 2.31 and reached 2.22 during cooling. The density of the pellets reached a maximum at 1200 °C, after which significant swelling occurred. Barzati [22], sintered 30 % Pu-MOX in Ar + 100 ppm O<sub>2</sub> and Ar + 500 ppm O<sub>2</sub>, and Kutty [18] used CO<sub>2</sub>. Such conditions are strongly oxidative and induce a large deviation from stoichiometry.

During the mild oxidative conditions reported here, the O/M of 11 % Pu-MOX at 1200 °C is kept at values higher than 2.00, but below 2.01, e.g. from Fig. 1 in Ref. [21]. Also during cooling, at 600 °C, either in CO/CO<sub>2</sub> or during the optional annealing in Ar/H<sub>2</sub>/H<sub>2</sub>O, the samples are expected to remain very slightly hyperstoichiometric ( $2.00 < \text{O/M} < 2.01$ ). On the other hand, sintering in conventional conditions in Ar/H<sub>2</sub>/H<sub>2</sub>O, sets an oxygen partial pressure giving a slightly hypo-stoichiometric composition (O/M  $\sim 1.99$ ). During cooling, the samples

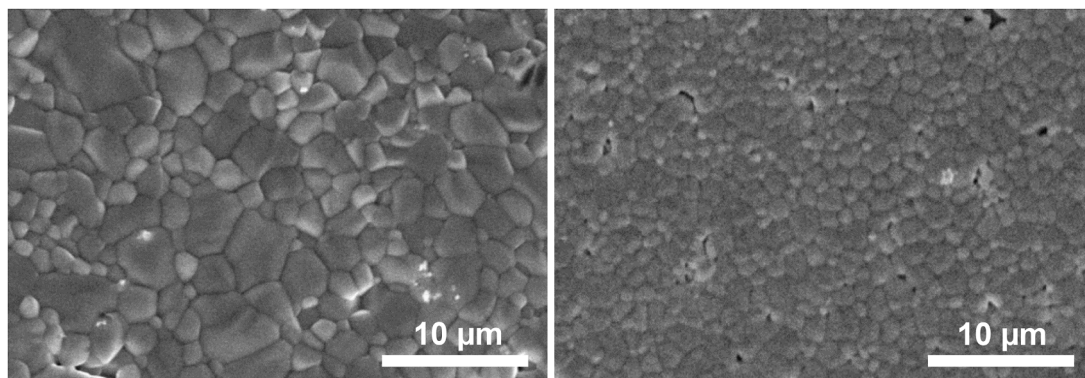


**Fig. 4.** SEM of the free surface of samples sintered at 1700 °C in Ar/H<sub>2</sub> (left) and at 1200 °C in CO/CO<sub>2</sub> (right).

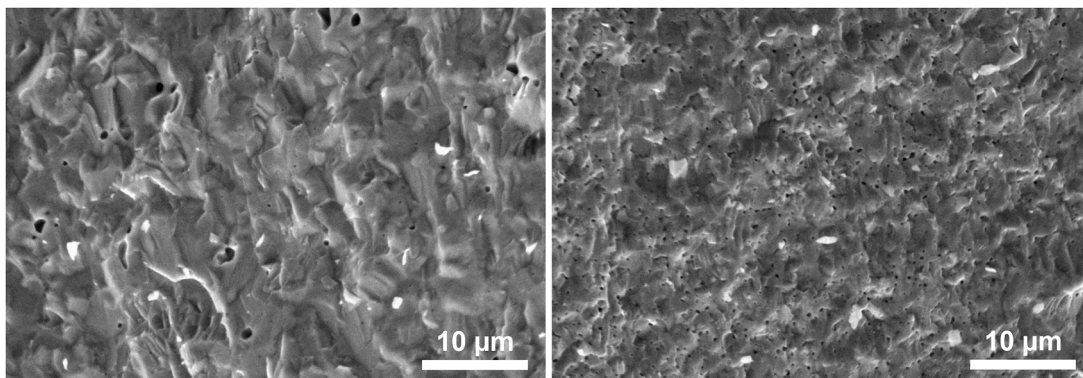


Fig. 5. SEM of the fracture surface of samples sintered at 1700 °C in Ar/H<sub>2</sub> (left) and at 1200 °C in CO/CO<sub>2</sub> (right).

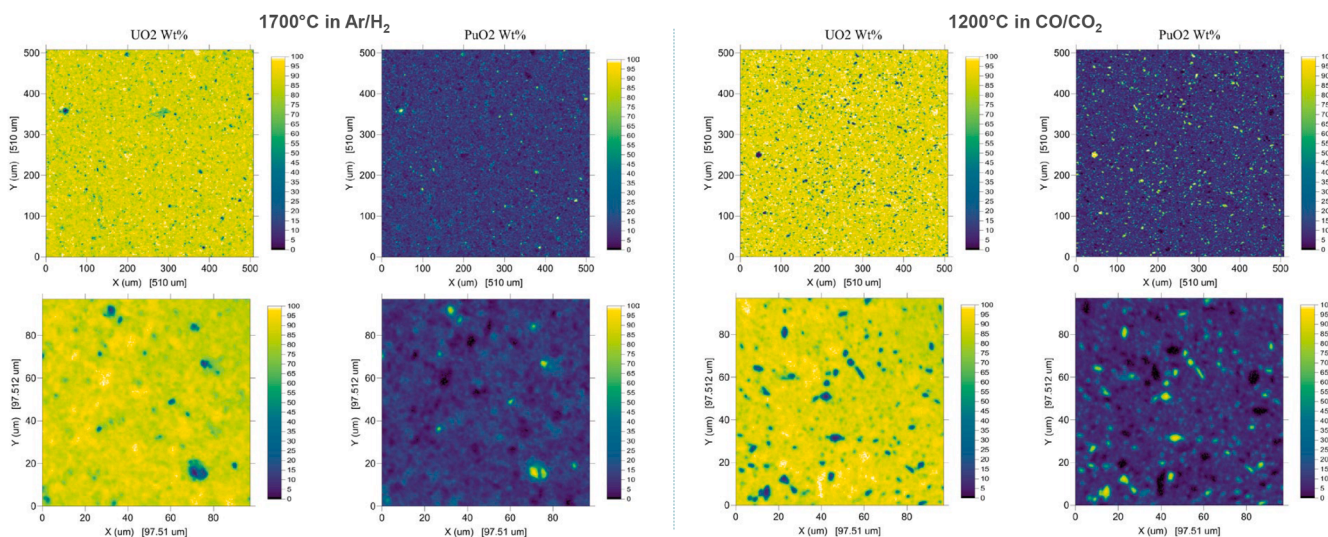


Fig. 6. Distribution of UO<sub>2</sub> and PuO<sub>2</sub> measured by EPMA on polished cross sections of samples sintered at 1700 °C in Ar/H<sub>2</sub> (left side) and at 1200 °C in CO/CO<sub>2</sub> (right side). Images in the bottom row are at a higher magnification (5x) than in the top row.

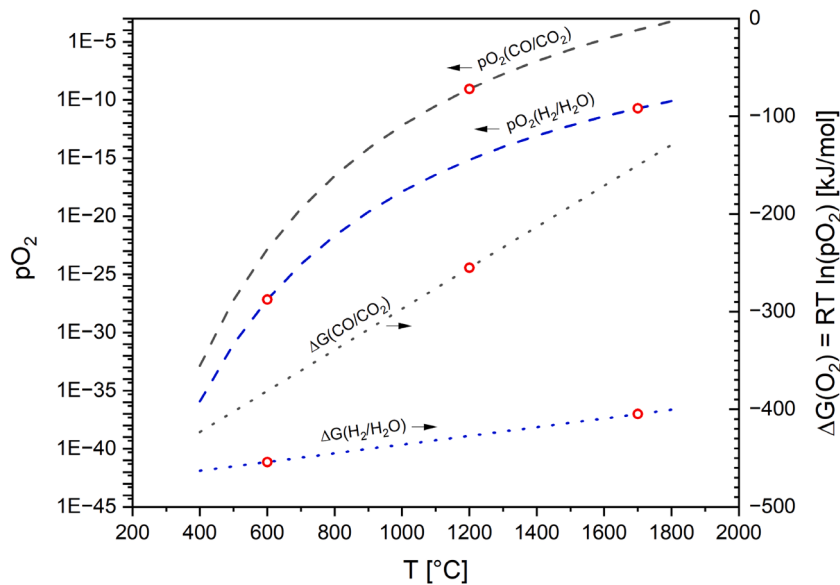


Fig. 7. Oxygen partial pressure and potential as a function of the temperature for the selected buffer couples: CO/CO<sub>2</sub> = 1/9 (black curves), and H<sub>2</sub>/H<sub>2</sub>O = 0.06/0.0012 (blue curves). The red dots specify the selected sintering and annealing conditions.

are expected to become slightly hyperstoichiometric, although with O/M very close to 2.00. These differences are not captured by the analysis methods used here, which have an estimated error of  $\pm 0.01$  O/M, so that we can only observe that, the samples are close-to stoichiometric for any conditions.

The low-temperature oxidative conditions used here are sufficient to achieve crack-free pellets with high relative density ( $\sim 95\%$ ) and a microstructure with closed porosity. However, the density, grain size, and degree of solid solution formation from  $\text{UO}_2$  and  $\text{PuO}_2$  end members are lower than those of the samples sintered for 4 h at  $1700^\circ\text{C}$ .

A typical and effective solution to increase such properties would be to increase the sintering temperature (the diffusion coefficients increase strongly with the temperature, following the Arrhenius law). However, at temperatures  $> 1200^\circ\text{C}$  in oxidative conditions, de-sintering may start to occur [21], although, if the reason for solarisation is the oxygen gas released during the reduction of U and Pu oxides at higher temperatures [21], solarisation may be less of a problem for the milder oxidative conditions studied here ( $2.00 < O/M < 2.01$ ).

An alternative would be to increase the dwell time at  $1200^\circ\text{C}$ . We can estimate the time that would be needed to achieve the desired grain size as follows: in isothermal conditions, the average grain size  $G$  grows with the time  $t$  as  $G^n - G_0^n = kt$ , with  $k$  the grain growth constant,  $n$  the grain growth exponent, and  $G_0$  the initial grain size at  $t = 0$ ; since  $G \gg G_0$  and assuming  $n = 2$  (the typical value for dense ceramic oxides), the average grain size has a time dependency of the type  $G \propto t^{1/2}$ . Thus, increasing the isothermal dwell time at  $1200^\circ\text{C}$  from 2 h to 8 h would double the grain size, allowing reaching a similar microstructure as the samples sintered for 4 h at  $1700^\circ\text{C}$  in reducing conditions. Longer dwell times, would also be beneficial for the homogenisation of  $\text{UO}_2$  and  $\text{PuO}_2$ . A high homogeneity in the U/Pu distribution is thought to give a better behaviour under reactor irradiation, by preventing the local formation of the high-burnup structure [25]. However, it is worth mentioning that increasing significantly the sintering duration would have a significant impact on the plant throughput.

Improvements in this aspect are also possible by a better homogenisation of the starting powder. The vibratory milling used here is not very efficient in terms of comminution (large particles of  $\text{PuO}_2$  are still present after milling the mixed powder, Fig. 1), and planetary milling is expected to give better results.

The use of powders with smaller particle size could also bring a further improvement: it has been recently shown that highly homogeneous  $\text{U}_{0.89}\text{Pu}_{0.11}\text{O}_2$  MOX with larger grain size is achieved in a conventional powder milling and reductive sintering process, only by replacing the typical ex-oxalate  $\text{PuO}_2$  powder by nano- $\text{PuO}_2$  powders obtained by hydrothermal precipitation [4]. Combining the mild oxidative sintering conditions in  $\text{CO}/\text{CO}_2$  and nano- $\text{PuO}_2$ , could give larger grain size and better homogeneity already at  $1200^\circ\text{C}$ .

## 5. Conclusions

Nuclear reactor  $\text{UO}_2$  fuel pellets are typically obtained in a high-temperature energy-intensive sintering process, where  $\text{H}_2$  gas is used to set reducing conditions. As an attempt to decrease the process energy and the cost and complexity of sintering furnaces, an alternative low-temperature oxidative sintering process for  $\text{UO}_2$  was developed and reported in the literature in the last decades. However, concerning (U, Pu) $\text{O}_2$  MOX fuel, less information is available in the open literature.

The results reported in this paper, show that the use of low-temperature, mildly oxidative conditions (2 h at  $1200^\circ\text{C}$  in  $\text{CO}/\text{CO}_2 = 1/9$ ) is an effective way to sinter (U,Pu) $\text{O}_2$  MOX pellets to high density and closed porosity. The obtained MOX pellets are crack-free and close to stoichiometric. The grain size and the density are still lower compared to the same samples sintered for longer time in typical reducing conditions (4 h at  $1700^\circ\text{C}$  in  $\text{Ar}/\text{H}_2$ ), as well as the degree of homogenisation of U and Pu. Optimisation of the process is expected to further improve the microstructural features. This may be achieved by increasing the

dwell time at  $1200^\circ\text{C}$ , improving the homogenisation of the powder mixture, or using smaller size  $\text{PuO}_2$  as starting powders.

## CRedit authorship contribution statement

**Jacobus Boshoven:** Writing – review & editing, Writing – original draft, Investigation. **Jean-François Vigier:** Writing – review & editing, Investigation, Formal analysis. **Philipp Pöml:** Writing – review & editing, Investigation. **Abibatou Ndiaye:** Writing – review & editing, Formal analysis, Conceptualization. **Bertrand Morel:** Writing – review & editing, Funding acquisition, Conceptualization. **Rudy J.M. Konings:** Writing – review & editing, Supervision, Funding acquisition, Conceptualization. **Karin Popa:** Writing – review & editing, Writing – original draft, Supervision, Investigation. **Marco Cologna:** Writing – review & editing, Writing – original draft, Supervision, Formal analysis.

## Declaration of competing interest

The authors declare that they have no known competing financial interests or personal relationships that could have appeared to influence the work reported in this article.

## Acknowledgements

The work was partially conducted under a Third Party Work (TPW) contract 35733. We are grateful to the JRC Analytical Services for chemical analysis, to Herwin Hein for TGA measurements, to Daniel Bouëxière for XRD measurements, and Ramon Carlos Marquez for SEM.

## Data availability

Data will be made available on request.

## References

- [1] F. La Lumia, L. Ramond, C. Pagnoux, P. Coste, F. Lebreton, J.R. Sevilla, G. Bernard-Granger, Dense and homogeneous MOX fuel pellets manufactured using the freeze granulation route, *J. Amer. Ceram. Soc.* (2020) 3020–3029.
- [2] S. Fehér, T. Reiss, A. Wirth, MOX fuel effects on the isotope inventory in LWRs, *Nucl. Eng. Des.* 252 (2012) 201–208.
- [3] L. Malerba, A. Al Mazouzi, M. Bertolus, M. Cologna, P. Efsing, A. Jianu, P. Kinnunen, K.-F. Nilsson, M. Rabung, M. Tarantino, Materials for sustainable nuclear energy: a European strategic research and innovation agenda for all reactor generations, *Energies* (2022) 1845.
- [4] J. Boshoven, A. Ndiaye, B. Morel, M. Cologna, J.-F. Vigier, R.C. Marquez, R.J. M. Konings, K. Popa, Homogeneous  $\text{U}_{0.89}\text{Pu}_{0.11}\text{O}_2$  mixed oxide by use of  $\text{PuO}_2$  nanopowders, *J. Nucl. Mater.* (2025) under review.
- [5] M. Cologna, 5.25 - Use of field assisted sintering for innovation in nuclear ceramics manufacturing. *Comprehensive Nuclear Materials (Second Edition)*, 2020, pp. 811–839.
- [6] K. Ando, Y. Oishi, Diffusion characteristics of actinide oxides, *J. Nucl. Sci. Technol.* (1983) 973–982.
- [7] H. Matzke, Lattice disorder and metal self-diffusion in non-stoichiometric  $\text{UO}_2$  and (U, Pu) $\text{O}_2$ , *J. Phys. Collo.* (1973) C9–317. -C9-325.
- [8] J. Williams, E. Barnes, R. Scott, A. Hall, Sintering of uranium oxides of composition  $\text{UO}_2$  to  $\text{U}_3\text{O}_8$  in various atmospheres, *J. Nucl. Mater.* (1959) 28–38.
- [9] N. Fuhrman, L.D. Hower JR, R.B. Holden, Low-temperature sintering of uranium dioxide, *J. Am. Ceram. Soc.* (1963) 114–121.
- [10] X.-D. Yang, J.-C. Gao, Y. Wang, X. Chang, Low-temperature sintering process for  $\text{UO}_2$  pellets in partially-oxidative atmosphere, *Trans. Nonferr. Metals Soc. China* (2008) 171–177.
- [11] T.R.G. Kutty, P.V. Hegde, K.B. Khan, U. Basak, S.N. Pillai, A.K. Sengupta, G.C. Jain, S. Majumdar, H.S. Kamath, D.S.C. Purushotham, Densification behaviour of  $\text{UO}_2$  in six different atmospheres, *J. Nucl. Mater.* (2002) 159–168.
- [12] H. Assmann, W. Dorr, N. Peeks, Control of  $\text{UO}_2$  microstructure by oxidative sintering, *J. Nucl. Mater.* (1986) 1–6.
- [13] IAEA-TECDOC-1686, Experiences and Trends of Manufacturing Technology of Advanced Nuclear Fuels, 2012.
- [14] E. González-Robles, V. Metz, D.H. Wegen, M. Herm, D. Papaioannou, E. Bohnert, R. Gretter, N. Müller, R. Nasyrow, W. de Weerd, T. Wiss, B. Kienzler, Determination of fission gas release of spent nuclear fuel in puncturing test and in leaching experiments under anoxic conditions, *J. Nucl. Mater.* (2016) 67–75.
- [15] D.G. Frost, P.A. Burr, E.G. Obbard, J. Velisek-Carolan, Controlling low temperature sintering of  $\text{UO}_{2+x}$ , *J. Nucl. Mater.* (2024) 155269.

- [16] I. Amato, R.L. Colombo, A.M. Protti, On a case of solarization during steam sintering of  $\text{UO}_2$  pellets, *J. Nucl. Mater.* (1963) 271–272.
- [17] W. Dörr, G. Maier, M. Peehs, Einstellung und charakterisierung der strukturgößen von LWR-Brennstoff, *J. Nucl. Mater.* (1982) 61–67.
- [18] T.R.G. Kutty, P.V. Hegde, K.B. Khan, S. Majumdar, D.S.C. Purushotham, Sintering studies on  $\text{UO}_2$ - $\text{PuO}_2$  pellets with varying  $\text{PuO}_2$  content using dilatometry, *J. Nucl. Mater.* (2000) 54–65.
- [19] T.R.G. Kutty, P.V. Hegde, R. Keswani, K.B. Khan, S. Majumdar, D.S.C. Purushotham, Densification behaviour of  $\text{UO}_2$ -50% $\text{PuO}_2$  pellets by dilatometry, *J. Nucl. Mater.* (1999) 10–19.
- [20] T.R.G. Kutty, K.B. Khan, P.V. Hegde, A.K. Sengupta, S. Majumdar, D.S.C. Purushotham, Densification behaviour and sintering kinetics of  $\text{PuO}_2$  pellets, *J. Nucl. Mater.* (2001) 120–128.
- [21] G.C.C. Miranda, L. Ramond, F. Lebreton, P. Signoret, P. Martin, A. Ndiaye, T. Gervais, G. Bernard-Granger, MOX fuel sintering under oxidizing conditions: a comprehensive study of the solarisation phenomenon, *J. Eur. Ceram. Soc.* (2023) 6373–6385.
- [22] S. Berzati, S. Vaudez, R.C. Belin, J. Léchelle, Y. Marc, J.-C. Richaud, J.-M. Heintz, Controlling the oxygen potential to improve the densification and the solid solution formation of uranium–plutonium mixed oxides, *J. Nucl. Mater.* (2014) 115–124.
- [23] D.R. Olander, *Fundamental Aspects of Nuclear Reactor Fuel Elements*, US DoE, 1976, p. 149.
- [24] M. Kato, K. Takeuchi, T. Uchida, T. Sunaoshi, K. Konashi, Oxygen potential of  $(\text{U}_{0.88}\text{Pu}_{0.12})\text{O}_{2\pm x}$  and  $(\text{U}_{0.7}\text{Pu}_{0.3})\text{O}_{2\pm x}$  at high temperatures of 1673–1873K, *J. Nucl. Mater.* 414 (2011) 120–125.
- [25] M. Le Guellec, F. Lebreton, L. Ramond, A. Ndiaye, T. Gervais, G. Bernard-Granger, Sintering investigations of a  $\text{UO}_2$ - $\text{PuO}_2$  powder synthesized using the freeze-granulation route, *Scripta materialia* (2010) 190–195.